Analytical Models for Phase-Modulation-Based Microwave Photonic Systems With Phase Modulation to Intensity Modulation Conversion Using a Dispersive Device

Hao Chi, Xihua Zou, and Jianping Yao, *Senior Member, IEEE, Member, OSA*

***Abstract*—Recently, optical phase modulation has been widely used in microwave photonics (MWP) systems, such as radio over fiber systems, photonic microwave filters, optical microwave and millimeter-wave signal generators, and optical subcarrier frequency up-converters. An optical phase-modulated signal can be converted to an intensity-modulated signal in a dispersive optical fiber. Due to the intrinsic nonlinearity of optical phase modulation, for linear applications such as microwave signal distribution and filtering, the modulation index should be kept small to minimize the unwanted modulation nonlinearity. However, for nonlinear applications such as microwave frequency multiplication and subcarrier frequency upconversion, the modulation index should be large to maximize the frequency multiplication and upconversion efficiency. In this paper, for the first time to our knowledge, we develop a thorough theoretical framework for the characterization of phase-modulation-based MWP systems, in which the phase modulation to intensity modulation conversion is realized using a dispersive fiber. Analytical models for the distributions of single-tone and two-tone microwave signals and for microwave frequency multiplication and subcarrier frequency upconversion are developed, which are verified by numerical simulations. The analytical models for single-tone and two-tone transmissions are further confirmed by experiments. The developed analytical models provide an accurate mathematical tool in designing phase-modulation-based MWP systems.**

***Index Terms*—Chromatic dispersion, microwave photonics (MWP), phase modulation (PM), radio-over-fiber (RoF), subcarrier modulation, wireless optical link.**

I. Introduction

THE GENERATION, distribution and processing of microwave signals in the optical domain has been a topic of research interest in the last two decades thanks to the many advantages such as low loss, light weight, broadband width, and immunity to electromagnetic interference offered by optics [1]. Recently, optical phase modulation (PM) has found many important applications in microwave photonics (MWP) systems, such as radio over fiber (RoF) systems, photonic microwave filters, optical microwave and millimeter-wave signal generators based on frequency multiplication, and optical subcarrier frequency up-converters [2]–[8]. The key advantage of using an optical phase modulator in a MWP system is that the phase modulator is not biased, which eliminates the bias drifting problem existing in a Mach–Zehnder modulator (MZM) based MWP system [9]. It is different from the use of an MZM in a MWP system where the intensity-modulated microwave signal can be directly detected using a photodetector (PD); the use of a phase modulator would generate a phase-modulated signal that has a constant envelope, which cannot be directly detected by a PD. To recover the microwave signal, the phase-modulated signal should be converted to an intensity-modulated signal, which can be realized by using a dispersive device to alter the phase relationships among the optical carrier and the optical sidebands, which has been demonstrated recently [10]. Therefore, in a phase-modulator-based MWP system, chromatic dispersion would be needed to perform the phase modulation to intensity modulation (PM-to-IM) conversion.

The applications of PM-based MWP systems can be generally classified into two categories: linear and nonlinear applications. The linear applications usually include photonic subcarrier signal distribution and photonic microwave filtering. In a PM-based system, as stated earlier, a phase-modulated signal would be converted to an intensity-modulated signal through PM-to-IM conversion in a dispersive optical fiber. The converted IM signal can be directly detected using a PD. This property has been recently utilized in a radio over fiber system for microwave/millimeter-wave signal generation and transmission [11]. In addition, the frequency response of a PM-based system has a notch at the dc, which can be utilized in a photonic microwave filter to suppress the baseband resonance, to achieve bandpass filtering [3]–[5], [12]. For linear applications, it is often required to assess the system performance, which is usually affected by the modulation nonlinearity. For example, in a radio over fiber distribution system, a good knowledge about the higher order harmonics (HoHs) and the third-order intermodulation distortion (IMD3) is vital to the design and analysis of the transmission system. Due to the intrinsic nonlinearity of optical phase modulation, for linear applications, the modulation index should be kept small in order to minimize

Manuscript received September 18, 2007; revised June 02, 2008. Current version published April 17, 2009. This work was supported in part by The Natural Sciences and Engineering Research Council of Canada (NSERC). The work of H. Chi was supported in part by the National Natural Science Foundation of China under 60871011 and in part by the Zhejiang Provincial Natural Science Foundation of China under Y1080184.

H. Chi is with the Department of Information and Electronic Engineering, Zhejiang University, Hangzhou, 310027 China, and also with the Microwave Photonics Research Laboratory, School of Information Technology and Engineering, University of Ottawa, Ottawa, ON K1N 6N5, Canada.

X. Zou and J. Yao are with the Microwave Photonics Research Laboratory, School of Information Technology and Engineering, University of Ottawa, Ottawa, ON K1N 6N5, Canada (e-mail: jpyao@site.uOttawa.ca).

Digital Object Identifier 10.1109/JLT.2008.2004595

the unwanted HoHs and/or intermodulation products (IMPs). However, for nonlinear applications, such as frequency multiplication and subcarrier frequency upconversion, the modulation index should not be too small to ensure a good frequency multiplication or upconversion efficiency. In a PM-based frequency multiplication or upconversion system, the desirable signal is just one of the generated HoHs or IMPs, which usually varies in amplitude along the dispersive optical link [6]–[8].

In the design and analysis of the PM-based MWP systems, either for linear or nonlinear applications, it is essential to know the power distributions of the fundamental harmonic and the HoHs and/or IMPs along the dispersive optical link. To the best of our knowledge, there is no analytical solution to this issue that has been provided up to now. In analyzing a linear PM-based MWP system, small signal approximation is widely used, in which only the first-order optical sidebands are considered. However, the treatment based on the small signal approximation does not provide the information about the HoHs and/or IMPs. A common way reported in literature to have a quantitative evaluation of the HoHs and/or IMPs is to include a number of optical sidebands in the numerical analysis; and the final solution is usually expressed as the sum of a finite series. In case that a large number of modulation sidebands need to be considered in the analysis to increase the calculation precision, this kind of treatment would become rather complicated and inconvenient. Recently, an exact analytical model for the distribution of the single-tone phase-modulated signal along a dispersive fiber link was developed by us [13]. In this paper, we propose for the first time, to the best of our knowledge, exact analytical models to characterize PM-based MWP systems for both linear and nonlinear applications. We will analyze the cases of the single-tone and two-tone subcarrier signal transmissions along dispersive link for linear applications. We will also analyze the cases of microwave frequency multiplication and subcarrier frequency upconversion for nonlinear applications. A unified theoretical framework is presented. Thanks to the application of the addition theorem for Bessel functions in the theoretical derivation, compact and closed-form expressions for the recovered microwave signals for different applications are developed. Since all optical sidebands are considered in the analysis, the developed analytical models are strict and accurate. The developed analytical models provide an accurate mathematical tool in designing PM-based MWP systems.

The remainder of the paper is organized as follows. In Section II, analytical models for the cases of single tone transmission, two tone transmission, microwave frequency multiplication, and subcarrier frequency upconversion are presented. The developed analytical models are evaluated by numerical simulation in Section III. The use of the analytical models for the analysis of different MWP systems is also presented in Section IVSection III.The experimental verification is presented in Section IV. In Section V, the limitation of the PM-based MWP systems is discussed and a conclusion is drawn.

II. Analytical Models

A. Single Tone Distribution

As shown in Fig. 1, a single tone microwave signal with an angular frequency ω_m is modulated upon the optical carrier via an optical phase modulator. The PM-to-IM conversion is realized by passing the phase-modulated optical signal through a length of dispersive optical fiber [10]. Due to the intrinsic modulation nonlinearity, HoHs with angular frequencies $k\omega_m$ $(k = 1, 2, 3, \ldots)$ would be generated even in the case of small signal modulation.

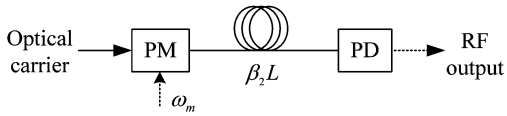

Fig. 1. Single tone transmission of a phase-modulated signal over a dispersive optical link.

The complex amplitude of the phase-modulated optical signal can be written as

$$E(t) = \exp[jm\cos(\omega_m t)] = \sum_{n=-\infty}^{\infty} j^n J_n(m)\exp(jn\omega_m t), \tag{1}$$

where m is modulation index, $J_n(\cdot)$ is the Bessel function of the first kind of order n. The modulation index m is related to the input signal amplitude V_s as $m = (V_s/V_\pi)\pi$, where V_π is the half-wave voltage of the phase modulator.

The dispersive link can be considered as a linear time invariant (LTI) system. For simplicity, we ignore the fiber-induced attenuation. The transfer function of the dispersive fiber with a length L is given as

$$H(j\omega) = \exp\left(j\frac{1}{2}\beta_2 L\omega^2\right). \tag{2}$$

where β_2 is the second-order dispersion coefficient of the optical fiber, ω is the offset angular frequence relative to the carrier, and the fiber-induced group delay and linear phase shift have been ignored for simplicity.

Therefore, the complex amplitude of the signal after experiencing the dispersive fiber can be expressed as

$$E_f(t) = \sum_{n=-\infty}^{\infty} j^n J_n(m)\exp(jn\omega_m t)\exp\left(j\frac{1}{2}\beta_2 L n^2\omega_m^2\right) = \sum_{n=-\infty}^{\infty}\Gamma_n. \tag{3}$$

The complex conjugate of $E_f(t)$ is given by

$$E_f^*(t) = \sum_{p=-\infty}^{\infty} j^{-p} J_p(m)\exp(-jp\omega_m t)\exp\left(-j\frac{1}{2}\beta_2 L p^2\omega_m^2\right) = \sum_{p=-\infty}^{\infty}\Gamma_p^*. \tag{4}$$

The signal contains infinite number of frequency components, with a specific phase shift introduced to each frequency component due to the fiber dispersion. The electrical signal at the output of the PD is proportional to the optical intensity, which is given by

$$i(t) = E_f(t)\cdot E_f^*(t). \tag{5}$$

The photodetection results in the beating between any two optical components, leading to the generation of different orders of electrical harmonic components. By observing (3) and (4), we find that the kth harmonic component $\exp(jk\omega_m t)$ with an angular frequency $k\omega_m$ can be expressed as $i_k(t) = \sum_{n=-\infty}^{\infty} \Gamma_{n+k}\Gamma_n^*$. Then we have

$$\begin{aligned} i_k(t) = \sum_{n=-\infty}^{\infty} & \{j^{n+k} J_{n+k}(m) \exp[j(n+k)\omega_m t] \\ & \times \exp\left[j\frac{1}{2}\beta_2 L(n+k)^2\omega_m^2\right] \\ & \times j^{-n} J_n(m) \exp(-jn\omega_m t) \\ & \times \exp\left(-j\frac{1}{2}\beta_2 L n^2\omega_m^2\right)\Big\}. \end{aligned} \tag{6}$$

In order to use the addition theorem for Bessel functions [14], we rearrange (6) as

$$\begin{aligned} i_k(t) = & j^k \exp\left(-j\frac{1}{2}\beta_2 L k^2\omega_m^2\right)\exp(jk\omega_m t) \\ & \times \sum_{n=-\infty}^{\infty} \{J_{n+k}(m)\exp[j\beta_2 L(n+k)k\omega_m^2\} \\ & \times \{J_n(m)\exp(j0)\}. \end{aligned} \tag{7}$$

The addition theorem for Bessel functions is expressed as

$$J_k(R)e^{jk\Omega} = \sum_{n=-\infty}^{\infty} \left[J_{k+n}(r)e^{j(k+n)\theta}\right]\left[J_n(r_0)e^{-jn\theta_0}\right] \tag{8}$$

where $R \cdot e^{j\Omega} = r \cdot e^{j\theta} - r_0 \cdot e^{j\theta_0}$.

By comparing (7) with (8), we have $r = m, \theta = \beta_2 L k\omega_m^2$, and $r_0 = m, \theta_0 = 0$. Then R and Ω are calculated to be $R = 2m\sin(\theta)/(2)$, and $\Omega = (1)/(2)(\pi+\theta)$. Therefore, $i_k(t)$ can now be written as

$$\begin{aligned} i_k(t) = & j^k \exp\left(-j\frac{1}{2}\beta_2 L k^2\omega_m^2\right)\exp(jk\omega_m t) \\ & \times J_k\left(2m\sin\frac{\theta}{2}\right)\exp\left[j\frac{1}{2}(\pi+\theta)k\right] \end{aligned} \tag{9}$$

which can be further simplified as

$$i_k(t) = (-1)^k J_k\left[2m\sin\left(\frac{1}{2}\beta_2 L k\omega_m^2\right)\right]\exp(jk\omega_m t). \tag{10}$$

Equation (10) is a closed-form expression that characterizes the variation of the kth order harmonic component along the dispersive fiber. Note that in the theoretical treatment, no small signal approximation was assumed and all optical modulation sidebands are included in the beating process. Therefore, the final solution is strict and accurate.

The overall electrical signal at the output of the PD is the sum of all the harmonic components, $i(t) = \sum_{k=0}^{\infty} i_k(t)$. For the first-order harmonic (FOH), if the condition for the small signal approximation, $m \ll 1$, is satisfied, we have

$$i_1(t) \approx -m\sin\left(\frac{1}{2}\beta_2 L\omega_m^2\right)\exp(j\omega_m t) \tag{11}$$

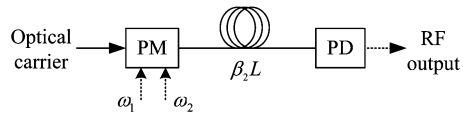

Fig. 2. Transmission of two tone phase modulated signal.

where $J_1(m) \approx m/2$ is applied. Equation (11) is the well known formula that gives the frequency response of a PM-based microwave transmission system with a dispersive optical link under linear modulation assumption [10].

B. Two Tone Transmission

In order to fully characterize the nonlinear property of the PM-based MWP system, the case of two-tone transmission should be considered [9]. For two input microwave signals with frequencies ω_1 and ω_2, as shown in Fig. 2, the output electrical signal would include infinite numbers of harmonics and intermodulation products (HIPs) with angular frequencies $k_1\omega_1 + k_2\omega_2$ $(k_1, k_2 = 0, \pm1, \pm2, \cdots)$ due to the modulation nonlinearity.

For simplicity, here we assume the two signals at ω_1 and ω_2 have the same modulation index m. The complex amplitude of the phase-modulated two-tone signal can be expressed as

$$\begin{aligned} E(t) &= \exp\{jm[\cos(\omega_1 t) + \cos(\omega_2 t + \varphi)]\} \\ &= \exp[jm(\omega_1 t)] \cdot \exp[jm(\omega_2 t + \varphi)] \\ &= \sum_{n=-\infty}^{\infty} j^n J_n(m)\exp(jn\omega_1 t) \\ &\quad \times \sum_{n=-\infty}^{\infty} j^n J_n(m)\exp(jn\varphi)\exp(jn\omega_2 t) \end{aligned} \tag{12}$$

where φ is the initial phase difference between the two microwave signals. We can reorganize (12) as

$$E(t) = \sum_{p=-\infty}^{\infty}\sum_{q=-\infty}^{\infty} j^{p+q} J_p J_q \exp(jq\varphi) \times \exp[j(p\omega_1 + q\omega_2)t] \tag{13}$$

where the arguments in Bessel functions are omitted for simplicity.

After the signal passes through the dispersive optical link, we have

$$\begin{aligned} E_f(t) &= \sum_{p=-\infty}^{\infty}\sum_{q=-\infty}^{\infty} \Big\{ j^{p+q} J_p J_q \exp(jq\varphi) \\ &\quad \times \exp[j(p\omega_1 + q\omega_2)t]\exp\left[j\frac{1}{2}\beta_2 L(p\omega_1 + q\omega_2)^2\right]\Big\} \\ &= \sum_{p,q} \Gamma_{p,q}. \end{aligned} \tag{14}$$

Its complex conjugate is given as

$$E_f^*(t) = \sum_{p=-\infty}^{\infty}\sum_{q=-\infty}^{\infty}\left\{ j^{-p-q}J_pJ_q\exp(-jq\varphi) \times \exp[-j(p\omega_1+q\omega_2)t] \times \exp\left[-j\frac{1}{2}\beta_2 L(p\omega_1+q\omega_2)^2\right]\right\} = \sum_{p,q}\Gamma_{p,q}^*. \quad (15)$$

The beating between any two optical components results in the generation of different orders of electrical HIPs. By observing (14) and (15), we find that the HIP term with angular frequency $k_1\omega_1 + k_2\omega_2$ can be expressed as $i_{k_1,k_2}(t) = \sum_{p,q}\Gamma_{p+k_1,q+k_2}\Gamma_{p,q}^*$. Then we have

$$i_{k1,k2} = j^{k_1+k_2}\exp(jk_2\varphi)\exp\left[-j\frac{1}{2}\beta_2 L(k_1\omega_1+k_2\omega_2)^2\right] \times \exp[j(k_1\omega_1+k_2\omega_2)t]\cdot T_1\cdot T_2 \quad (16)$$

where

$$T_1 = \sum_{p=-\infty}^{\infty} J_pJ_{p-k_1}\exp\left[j\beta_2 L\left(k_1\omega_1^2+k_2\omega_1\omega_2\right)p\right] \quad (17)$$

$$T_2 = \sum_{q=-\infty}^{\infty} J_qJ_{q-k_2}\exp\left[j\beta_2 L\left(k_2\omega_2^2+k_1\omega_1\omega_2\right)q\right]. \quad (18)$$

Again, using the addition theorem, T_1 and T_2 can be simplified as

$$T_1 = j^{k_1}\exp\left(j\frac{1}{2}k_1\theta_1\right)J_{k_1}(2m\sin\theta_1 2) \quad (19)$$

where $\theta_1 = \beta_2 L(k_1\omega_1^2 + k_2\omega_1\omega_2)$, and

$$T_2 = j^{k_2}\exp\left(j\frac{1}{2}k_2\theta_2\right)J_{k_2}\left(2m\sin\frac{\theta_2}{2}\right) \quad (20)$$

where $\theta_2 = \beta_2 L(k_2\omega_2^2 + k_1\omega_1\omega_2)$.

Therefore, we have the final expression according to (16), (19) and (20) as

$$i_{k_1,k_2}(t) = (-1)^{k_1+k_2}\exp(jk_2\varphi)J_{k_1}\left(2m\sin\frac{\theta_1}{2}\right) \times J_{k_2}\left(2m\sin\frac{\theta_2}{2}\right)\exp[j(k_1\omega_1+k_2\omega_2)t]. \quad (21)$$

Note that (21) gives the full characterization of the generation and distribution of an arbitrary order of HIP along the dispersive optical link. In the analysis of the spurious-free dynamic range (SFDR) of an RF system, the concerned HIPs include the FOH, ω_1 ($k_1 = 1, k_2 = 0$) or ω_2 ($k_1 = 0, k_2 = 1$), and the third-order inter-modulation products (IMP3) $2\omega_1 - \omega_2$ ($k_1 = 2, k_2 = -1$) or $2\omega_2 - \omega_1$ ($k_1 = -1, k_2 = 2$).

Under small signal approximation, we can obtain the expressions for the power of the FOH and the IMP3,

$$P_{1,0} = |i_{1,0}|^2 \approx \left|m\sin\left(\frac{1}{2}\beta_2 L\omega_1^2\right)\right|^2 \quad (22)$$

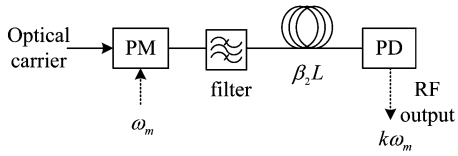

Fig. 3. Schematic diagram showing frequency multiplication based on an optical phase modulator, where the optical carrier at the output of the phase modulator is eliminated by the optical filter.

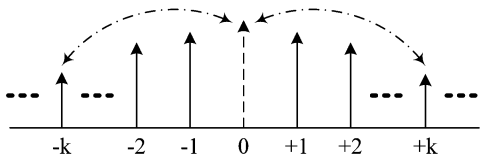

Fig. 4. Beating between the optical carrier and the $\pm k$th order optical modulation sidebands.

and

$$P_{2,-1} = |i_{2,-1}|^2 \approx \left|\frac{1}{2}m^3\sin^3\left(\frac{1}{2}\beta_2 L\omega_1^2\right)\right|^2 \quad (23)$$

where in (22) and (23), $|\omega_1 - \omega_2| \ll \omega_1$ is assumed, and $J_n(x) \approx x^n/(2^n n!)$ is applied.

Due to $P_{2,-1} = P_{1,0}$ at the third-order intercept point, we can obtain the input third-order intercept point (IIP3) as

$$m_{IP3} = \sqrt{2}\left|\sin\left(\frac{1}{2}\beta_2 L\omega_1^2\right)\right|^{-1}. \quad (24)$$

C. Frequency Multiplication

Optical PM has also found applications in millimeter-wave signal generation based on frequency multiplication [6], thanks to the advantages such as low loss and free of bias drift. The schematic diagram of a PM-based frequency multiplication scheme is shown in Fig. 3, where an optical filter is placed at the output of the phase modulator to block the optical carrier and to bypass the optical modulation sidebands.

Since the optical carrier is eliminated, the generated kth harmonic component $i_k^{\text{cs}}(t)$ should be the $i_k(t)$ as in (10) with the beating results between the optical carrier and the $\pm k$th order sidebands being removed. Therefore, $i_k^{\text{cs}}(t)$ can be expressed as $i_k^{\text{cs}}(t) = i_k(t) - \overline{i_k}(t) = i_k(t) - (\Gamma_0\Gamma_{-k}^* + \Gamma_k\Gamma_0^*)$, where $\overline{i_k}(t)$ is the beating results between the optical carrier and the $\pm k$ th order sidebands, as shown in Fig. 4, which is expressed as

$$\overline{i_k}(t) = \Gamma_0\Gamma_{-k}^* + \Gamma_k\Gamma_0^* = j^k J_0(m)J_k(m)\exp(jk\omega_m t) \times \left[\exp\left(j\frac{1}{2}\beta_2 Lk^2\omega_m^2\right) + (-1)^k\exp\left(j\frac{1}{2}\beta_2 Lk^2\omega_m^2\right)\right]. \quad (25)$$

For a special case where the chromatic dispersion is zero, we can obtain

$$i_k^{\text{cs}}(t) = \begin{cases} 0, & \text{for odd } k \\ -2j^k J_0(m)J_k(m)\exp(jk\omega_m t), & \text{for even } k. \end{cases} \quad (26)$$

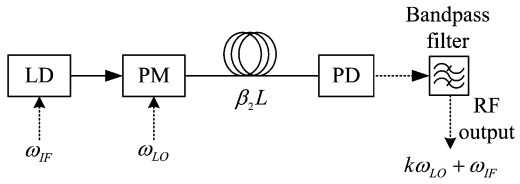

Fig. 5. Subcarrier frequency upconversion using an optical phase modulator.

According to (26), we can see that only even-order harmonics would be generated if the transmission system is dispersion free. In addition, for the case of small signal modulation, the amplitudes of the generated harmonics with orders greater than 2 is much smaller that that of the second-order harmonic and can be neglected, which will be clarified in the next section.

D. Frequency Upconversion

The scheme to implement subcarrier frequency upconversion using a phase modulator is shown in Fig. 5. The intermediate frequency (IF) signal $\omega_{\rm IF}$ is directly modulated on the laser diode (LD). Optical mixing is implemented in the optical phase modulator, to which a local oscillator (LO) $\omega_{\rm LO}$ is added [7], [8]. The upconverted signal $k\omega_{\rm LO}+\omega_{\rm IF}$ (typically $k=1$ or 2) is obtained after photodetection.

Since we focus on the nonlinear mixing process in the phase modulator, the modulation nonlinearity in the direct modulation at the LD is ignored. In this case, the complex amplitude of the signal at the output of the phase modulator is given by

$$\begin{aligned} E(t) &= [1+m_1\cos(\omega_{\rm IF}t)]\exp[jm_2\cos(\omega_{\rm LO}t)] \\ &= \left\{1+\frac{m_1}{2}[\exp(j\omega_{\rm IF}t)+\exp(-j\omega_{\rm IF}t)]\right\} \\ &\quad\times\sum_{n=-\infty}^{\infty} j^n J_n(m_2)\exp(jn\omega_{\rm LO}t) \\ &= \sum_{n=-\infty}^{\infty} j^n J_n(m_2)\cdot\{\exp(jn\omega_{\rm LO}t) \\ &\quad+\frac{m_1}{2}\exp[j(n\omega_{\rm LO}+\omega_{\rm IF})t] \\ &\quad+\frac{m_1}{2}\exp[j(n\omega_{\rm LO}-\omega_{\rm IF})t]\Big\} \end{aligned} \tag{27}$$

where m_1 and m_2 are the modulation indices of the IF signal and the LO, respectively. After experiencing the dispersion in the fiber, we have

$$\begin{aligned} E_f(t) &= \sum_{n=-\infty}^{\infty} j^n J_n(m_2) \\ &\quad\cdot\left\{\exp(jn\omega_{\rm LO}t)\cdot\exp\left(j\frac{1}{2}\beta_2 L n^2\omega_{\rm LO}^2\right)\right. \\ &\quad+\frac{m_1}{2}\exp[j(n\omega_{\rm LO}+\omega_{\rm IF})t] \\ &\quad\cdot\exp\left[j\frac{1}{2}\beta_2 L(n\omega_{\rm LO}+\omega_{\rm IF})^2\right] \\ &\quad+\frac{m_1}{2}\exp\left[j(n\omega_{\rm LO}-\omega_{\rm IF})t\right] \\ &\quad\left.\cdot\exp\left[j\frac{1}{2}\beta_2 L(n\omega_{\rm LO}-\omega_{\rm IF})^2\right]\right\} \\ &= \sum_{n=-\infty}^{\infty}\{\Gamma_{n\omega_{\rm LO}}+\Gamma_{n\omega_{\rm LO}+\omega_{\rm IF}}+\Gamma_{n\omega_{\rm LO}-\omega_{\rm IF}}\} \end{aligned} \tag{28}$$

Its complex conjugate is

$$E_f^*(t)=\sum_{n=-\infty}^{\infty}\left\{\Gamma_{n\omega_{\rm LO}}^*+\Gamma_{n\omega_{\rm LO}+\omega_{\rm IF}}^*+\Gamma_{n\omega_{\rm LO}-\omega_{\rm IF}}^*\right\}. \tag{29}$$

The beating between any two optical components results in the generation of different orders of HIPs. By observing (27) and (28), we find that the HIP term with angular frequency $k\omega_{\rm LO}+\omega_{\rm IF}$ can be expressed as

$$\begin{aligned} i_{k\omega_{\rm LO}+\omega_{\rm IF}}(t) &= \sum_{n=-\infty}^{\infty}\left\{\Gamma_{n\omega_{\rm LO}}^*\Gamma_{(n+k)\omega_{\rm LO}+\omega_{\rm IF}}\right. \\ &\quad\left.+\Gamma_{(n+k)\omega_{\rm LO}}\Gamma_{n\omega_{\rm LO}-\omega_{\rm IF}}^*\right\}. \end{aligned} \tag{30}$$

According to the derivations in the Appendix I, by using the addition theorem for Bessel functions, we can obtain

$$\begin{aligned} i_{k\omega_{\rm LO}+\omega_{\rm IF}}(t) &= (-1)^k m_1\cos\left[\frac{1}{2}\beta_2 L\left(k\omega_{\rm LO}\omega_{\rm IF}+\omega_{\rm IF}^2\right)\right] \\ &\quad\times J_k(R)\cdot\exp[j(k\omega_{\rm LO}+\omega_{\rm IF})t] \end{aligned} \tag{31}$$

where $R=2m_2\sin[\beta_2 L(\omega_{\rm LO}\omega_{\rm IF}+k\omega_{\rm LO}^2)/2]$. It can be seen that (31) fully characterizes the frequency upconverted signals at different orders at different locations of the dispersive optical link.

III. Simulation Results

The presented analytical models are utilized to analyze the PM-based MWP systems for applications including single-tone transmission, two-tone transmission, microwave frequency multiplication, and subcarrier frequency upconversion. The analyses are verified by numerical simulations.

A. Single-Tone Transmission

Single-tone transmission over a dispersive RoF link is considered, in which an input microwave signal at 10 GHz is applied to the phase modulator. The distribution of the FOH along the dispersive optical link is first investigated. Fig. 6 shows the output power of the FOH versus the dispersion with different modulation indices, where the harmonic power $|i_k|^2$ is normalized to m^2. For comparison, the result given by the small signal approximation is also plotted in Fig. 6. It is shown that an increase in the modulation index would lead to a decrease in the normalized power (i.e., the efficiency of the transmission system is reduced) due to the stronger modulation nonlinearity. More importantly, the maximum power point along the dispersive link also changes in the case of large modulation index, as can be seen from the curve for $m=\pi/2$ in Fig. 6. Fig. 7(a) shows the frequency response for different modulation indices at $\beta_2 L=800$ ps^2. Fig. 7(b) gives the dependence of the normalized peak power on the input signal power, which demonstrates the 1-dB compression point is $m=\pi/6.6$, corresponding to an input power of around 10.3 dBm. Here, we assume the half-wave voltage V_π and the input impedance $Z_{\rm in}$ of the phase modulator are 4.8 V and 50 Ω, respectively. The input signal power P is related to the modulation index m as $P=m^2V_\pi^2/(\pi^2 Z_{\rm in})$. The results given here match well with the previous results reported in [12]. The 1-dB compression point roughly gives the upper-limit of the allowed input signal power.

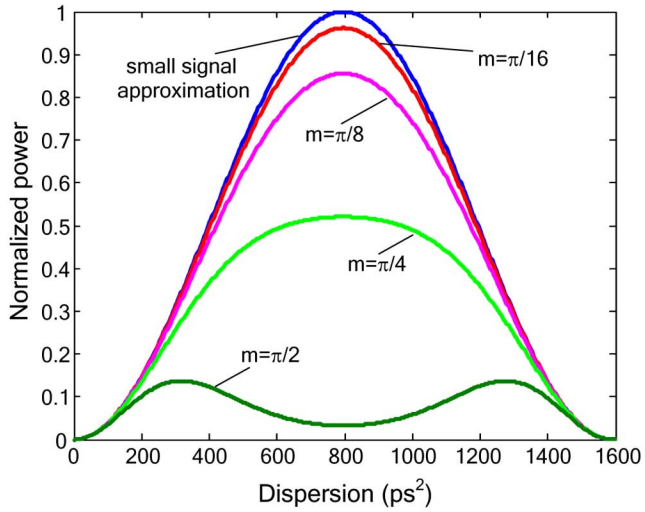

Fig. 6. Power variation of the FOH along the dispersive optical link with different modulation indices (10 GHz).

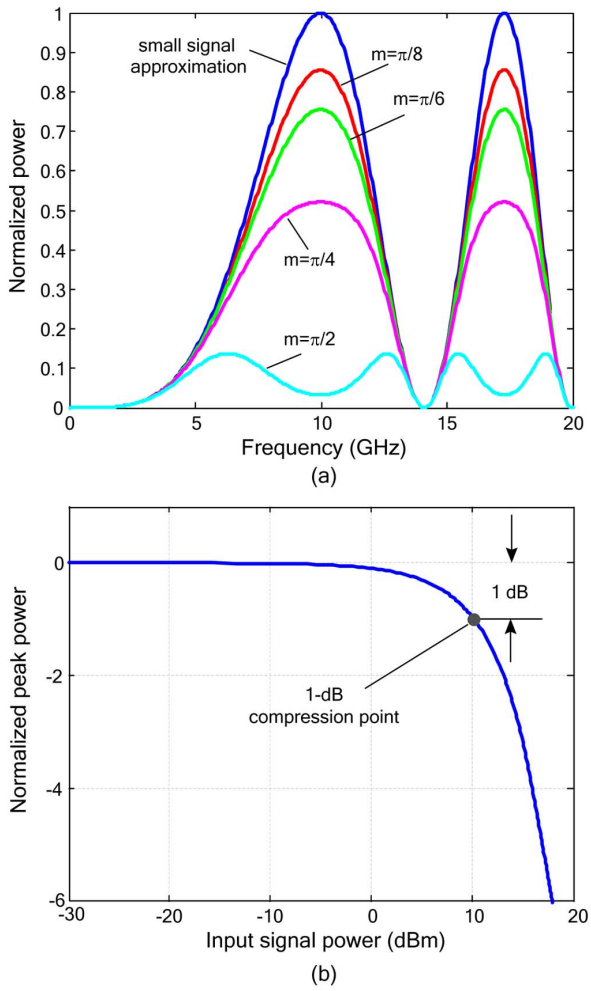

Fig. 7. (a) Normalized frequency response for different modulation indices at $\beta_2 L = 800\text{ps}^2$; (b) normalized peak power versus input signal power.

Then, we investigated the power distributions of different orders of harmonics along the dispersive link. Fig. 8(a) and (b) shows the normalized powers of three harmonics (first-, second-, and third-order) along the dispersive link with $m = \pi/2$ and $m = \pi$. Numerical simulation based on fast Fourier transform (FFT) is also implemented to verify the developed theoretical model; results are also shown in Fig. 8. To achieve a high calculation precision in the simulation, we set the frequency range of the FFT as 40 times of the input signal frequency, which means that the first twenty modulation sidebands are included in the beating process. It is shown that the results predicted by the theoretical model perfectly match with the simulation results, which proves the correctness of the derived formula.

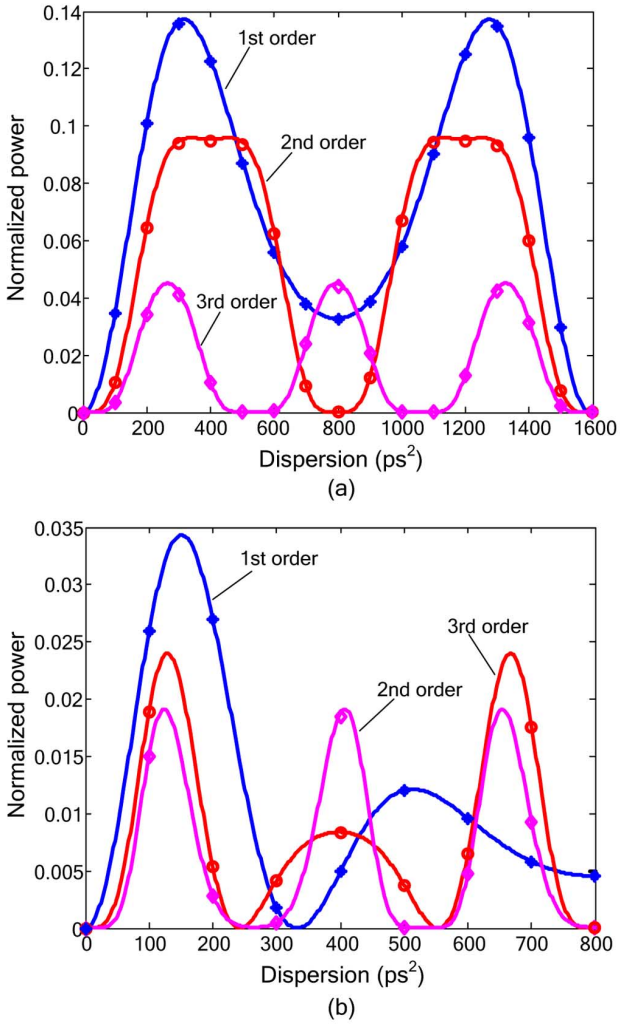

Fig. 8. Power distributions of the first-, second- and third-order harmonics versus the dispersion in the optical link, where solid curves are theoretical predictions, the stars, circles and diamonds denote numerical simulation results. (a) $m = \pi/2$; (b) $m = \pi$.

B. Two-Tone Transmission

Two-tone transmission over a dispersive optical link is then considered. The two tones at $f_1 = 10$ GHz and $f_2 = 10.9$ GHz, are sent to the phase modulator. The power distributions of the generated FOH component at f_1 and the IMP3 at $2f_1 - f_2$ are evaluated. Fig. 9 shows the distributions of the normalized power of the generated FOH and the IMP3 along the dispersive optical link with $m = \pi/2$. Numerical results are also shown

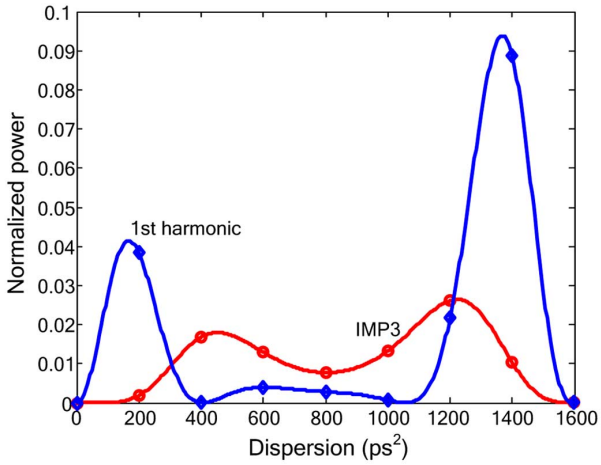

Fig. 9. Power variations of the FOH and the IMP3 along the dispersive optical link with $m = \pi/2$, where solid curves are theoretical predictions, the circles and diamonds denote numerical simulation results.

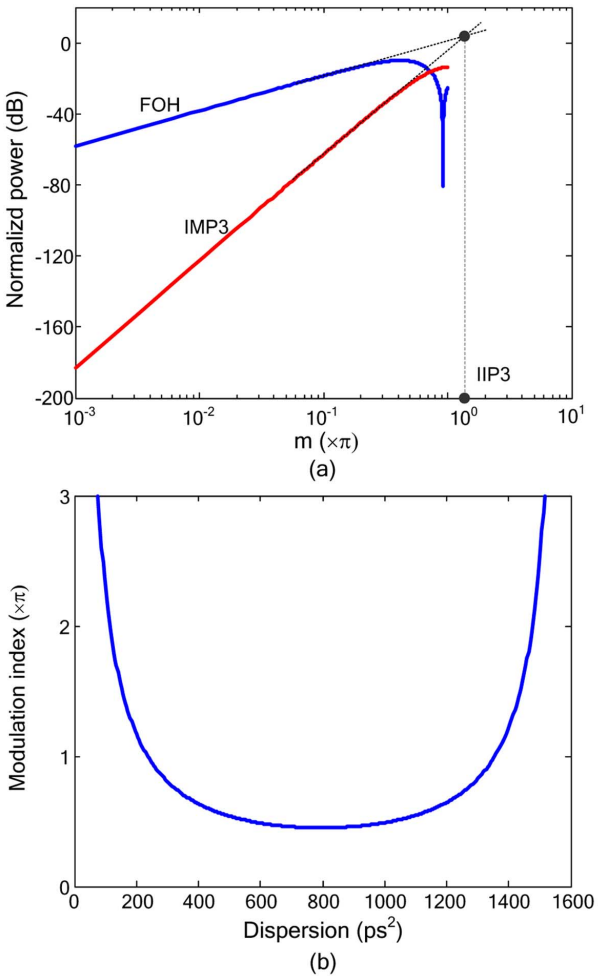

Fig. 10. (a) Power of the FOH and the IMP3 versus the modulation index, where solid curves are theoretical predictions, the circles and diamonds denote numerical simulation results (200 ps^2); (b) IIP3 in modulation index versus dispersion.

in Fig. 9, which match well with the calculated results based on the given model.

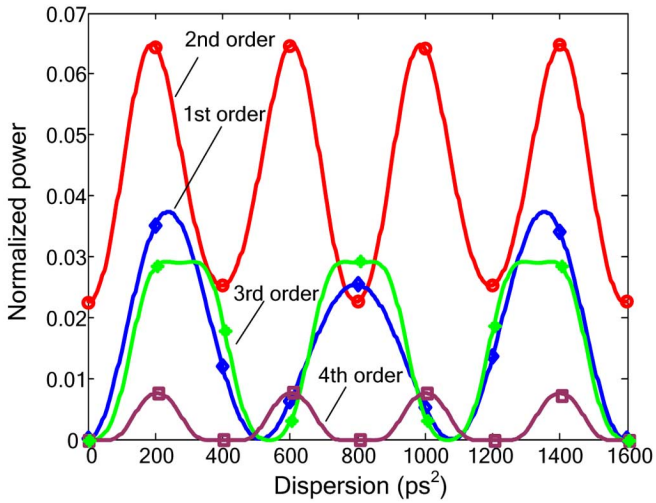

Fig. 11. Power distributions of the first to fourth harmonic components along dispersive optical link, where the solid curves show theoretical results based on the analytical models, the circles, diamonds, stars and squares show the simulation results (10 GHz, $m = \pi/2$).

Then, the IIP3 of the phase-modulated transmission system is investigated. Fig. 10(a) gives the normalized power of the FOH and the IMP3 versus the modulation index at a dispersion of 200 ps^2 in log scale, with the definition of the IIP3 shown in the figure. Fig. 10(b) shows the IIP3 versus dispersion based on (24). Note that a larger IIP3 means a higher dynamic range. However, by comparing Fig. 10(b) with Fig. 9, we find that the dispersion point with a maximum IIP3 corresponds to the lowest normalized output power. Therefore, there is a trade-off between the normalized output power and the system dynamic range, which should be taken into account in the system design.

C. Frequency Multiplication

To implement frequency multiplication, the optical carrier should be filtered out by a narrow band optical filter. Fig. 11 shows the power distributions of the first to fourth orders of harmonic components along the dispersive optical link with $m = \pi/2$. It is found that the power of the generated harmonics varies with the accumulated dispersion. In addition, the variation period of the first order harmonic is roughly the same as that of the third order harmonic, and the variation period of the second order harmonic is roughly the same as that of the fourth order harmonic. It is interesting to note that with zero dispersion, there is only a second order harmonic, the first, the third and the fourth harmonics are all suppressed. This finding agrees well with the derivation in (26). Based on (26), the odd-order harmonics are null with zero dispersion, while the magnitudes of the even-order harmonics are proportional to $J_k(m)$. As we know, for a small modulation index m (e.g., $m \leq \pi/2$), we have $J_k(m) \ll J_2(m)$, where $k = 4, 6, 8, \ldots$, as can be found from Fig. 12. Therefore, only the second order harmonic is generated when the system is dispersion free.

On the other hand, in a system without dispersion compensation, more than one harmonic component would be generated. Therefore, to realize frequency doubling without other fre-

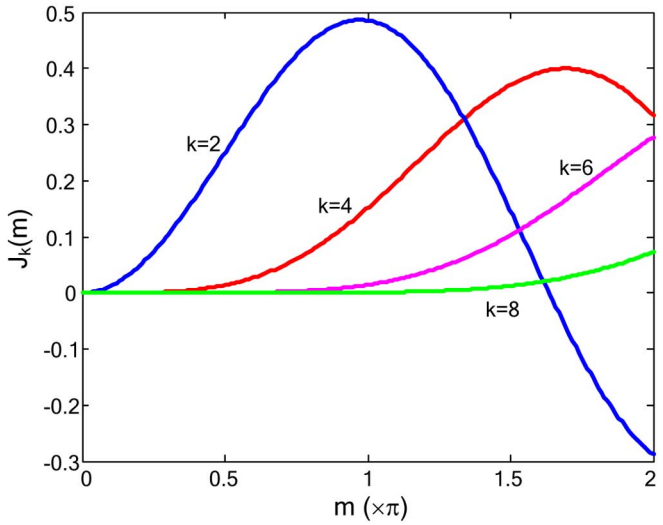

Fig. 12. Bessel function of the first kind with even order $J_k(m)$.

quency components, dispersion compensation is required. This finding also agrees with the previous experimental results in [6]. For the case of larger modulation index ($m > \pi/2$), higher even-order harmonics appears, which can be found from Fig. 12. In this case, if one of the higher even-order harmonics, such as the forth-order harmonic, is concerned, electrical bandpass filter or microwave photonic bandpass filter has to be used to extract the required harmonic component.

D. Subcarrier Frequency upconversion

An intensity-modulated IF signal at $\omega_{\rm IF}$ can be up-converted to $k\omega_{\rm LO}+\omega_{\rm IF}, k = 1, 2, 3, \ldots$ in a system as shown in Fig. 5. In the evaluation, we assume that $\omega_{\rm IF} = 2\pi \times 30$ MHz and $\omega_{\rm LO} = 2\pi \times 10$ GHz. Fig. 13(a) and (b) shows the distributions of the normalized powers of the upconverted signals at $k\omega_{\rm LO} + \omega_{\rm IF}$ (k =1, 2, and 3) along the dispersive link with $m = \pi/2$ and π. It is found that the powers of different orders of the upconverted signal are all null at the zero dispersion. This is understandable since a direct detection of a phase-modulated signal would not recover any signals except a dc. Therefore, to obtain the frequency up-converted signals, chromatic dispersion in the optical link is necessary. As can be seen from Fig. 13, the dispersion values to achieve maximum output powers are different for different orders of the upconverted signals. In addition, a change in the modulation index would result in the change in the power distribution profile of the upconverted signal along the dispersive link. For example, for the first-order upconverted signal $\omega_{\rm LO} + \omega_{\rm IF}$, when the modulation index is $\pi/2$, the optimum dispersion that leads to a maximum output power in the optical link is around 300 ps^2; while for $m = \pi$, the dispersion that leads to a maximum power is changed to be around 150 ps^2. Therefore, in the design of a subcarrier frequency upconversion system, both the modulation index and the fiber dispersion should be considered to achieve the maximum output power. Again, numerical results are also shown Fig. 13, which match well with the calculated results based on the analytical model.

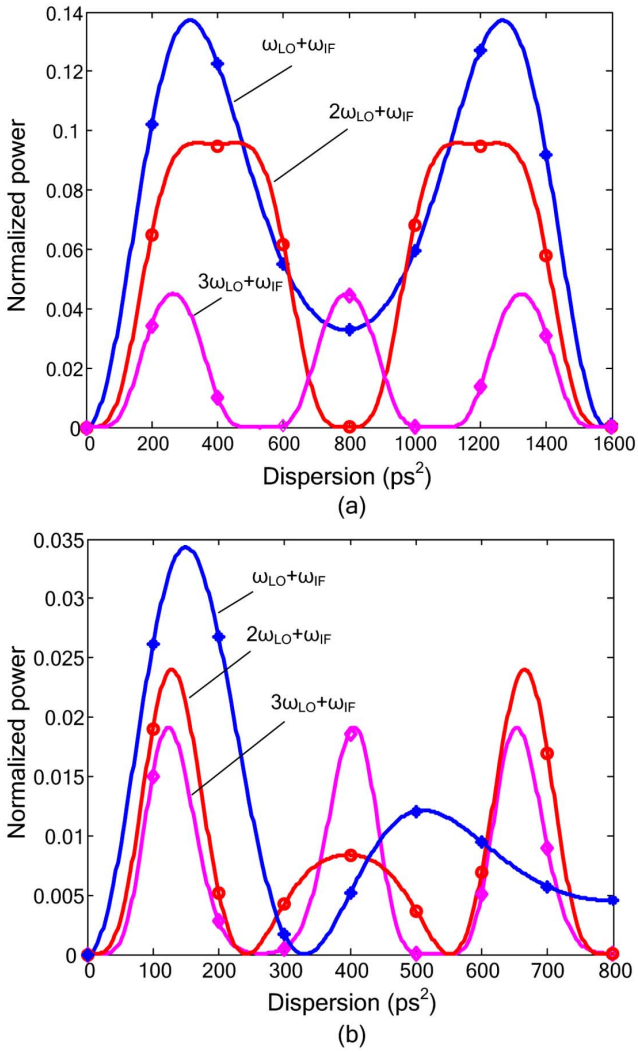

Fig. 13. Power distributions of the first-, second- and third-order upconverted signals along the dispersive optical link, where the solid curves show the theoretical results based on the analytoical model, the stars, circles and diamonds denote the simulation results for (a) $m = \pi/2$; and (b) $m = \pi$. ($f_{\rm LO} = 10$ GHz, $f_{\rm IF} = 30$ MHz).

IV. Experiments

To further confirm the analytical models, experiments for single-tone and two-tone transmissions are conducted. The experimental setup is shown in Fig. 14. As can be seen a microwave signal generated from a microwave generator (Agilent E8254A) is amplified before applied to a JDS-Uniphase phase modulator. The optical signal from the phase modulator is then sent to a length of single-mode-fiber (SMF), serving as a dispersive device to perform PM-to-IM conversion. The microwave signal and its harmonics are then detected by a PD (New Focus 1014) with their power spectra analyzed by a spectrum analyzer (Agilent E4448A).

In the experiments, the SMF with different lengths is used to emulate the optical links with different dispersions. As listed in Table I, four different dispersions are provided by the SMF with four different lengths. Although the fiber loss due to the length difference is different, we are able to tune the output power of

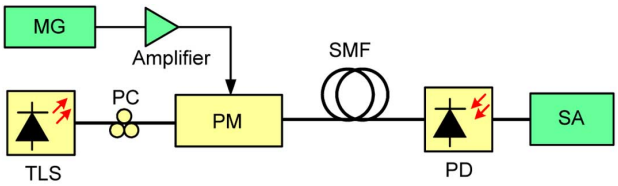

Fig. 14. Experimental setup used to verify the analytical models. MG: microwave generator; TLS: tunable laser source; PM: phase modulator; SMF: single-mode fiber; PD: photodetector; SA: spectrum analyzer.

TABLE I
DISPERSIONS OF THE SMF WITH FOUR DIFFERENT LENGTHS

Fiber length (km)	10.6	20	34.8	49.8
Dispersion (ps^2)	229.67	433.3	754	1057.8

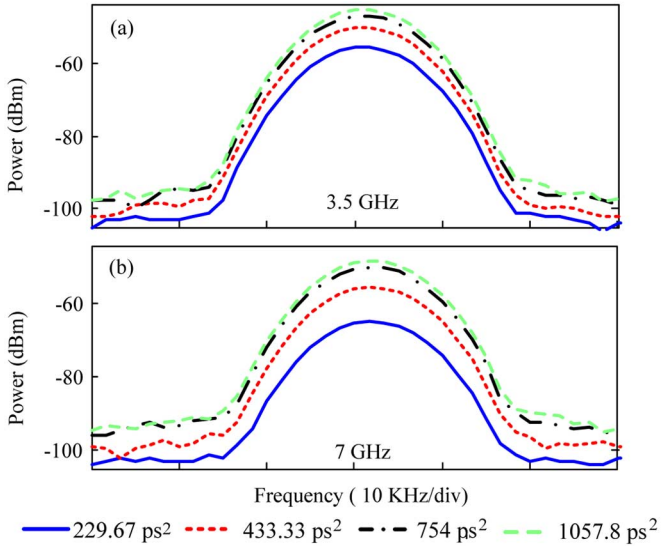

Fig. 15. Measured power spectra for (a) the FOH and (b) the SOH in the single-tone transmission test.

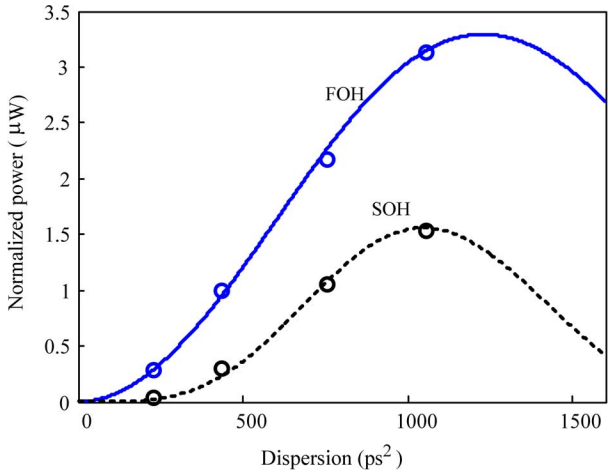

Fig. 16. Comparison between the measured (circles) and the theoretical (solid and dotted lines) power distributions in the single-tone transmission test.

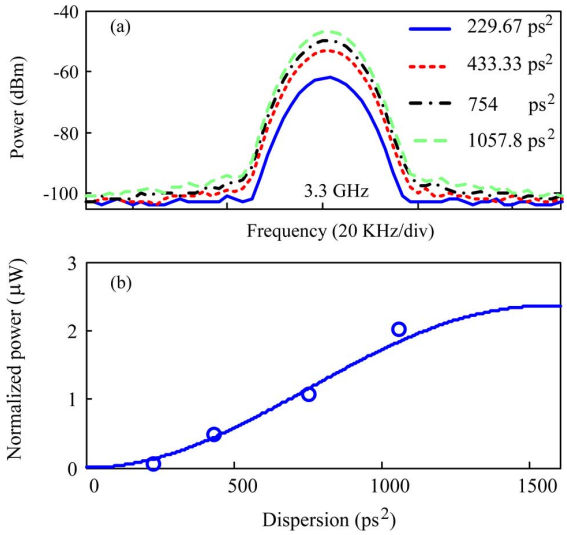

Fig. 17. (a) Measured power spectra and (b) normalized power distribution for the FOH in two-tone transmission.

the tunable laser source (TLS, Yokogawa AQ 2201) to compensate for the loss, which ensures an identical loss for the four different fiber lengths.

For the single-tone transmission test, a microwave signal with a frequency of 3.5 GHz is applied to the phase modulator with the modulation depth adjusted to be π. The measured power spectra for the FOH (3.5 GHz) and the SOH (7 GHz) are shown in Fig. 15. Since the harmonic power distributions analyzed in Section III were normalized to m^2, a similar normalization operation is performed for the measured microwave powers for the simplicity of comparison. After being normalized, in Fig. 16 the measured powers for both the FOH and the SOH agree well with their theoretical values obtained based on (10). The analytical model for single-tone transmission is verified.

Then the two-tone transmission is experimentally investigated. Two microwave signals at 3.3 and 3.5 GHz generated by a microwave generator (Agilent E8254A) and a network analyzer (Agilent E8364A) are combined by a microwave combiner and amplified before being sent to the phase modulator. In the experiment, the modulation depth is controlled to be $\pi/2$, to ensure that the microwave amplifier is operating in the linear region. Therefore, the nonlinearity of the entire system can be considered to be generated by the phase modulator only. The spectra and normalized power spectra of the generated FOH (3.3 GHz) are shown in Fig. 17, while those of the IMP3 (3.1 GHz) are illustrated in Fig. 18. As can be seen the measured powers of both the FOH and the IMP3 for the SMF with four different dispersions follow the theoretical distributions obtained based on the analytical model in (21).

V. DISCUSSIONS AND CONCLUSION

Optical phase modulation provides an attractive alternative to optical intensity modulation for MWP applications. As we have discussed in Section II, in a PM-based MWP system, the PM-to-IM conversion is achieved when a phase modulated signal is propagating in a dispersive optical link. Note that, the PM-to-IM conversion can also be realized using a frequency discriminator that has an interferometric structure [9], [15]. A major drawback related to the use of PM in a MWP system, with PM-to-IM conversion achieved

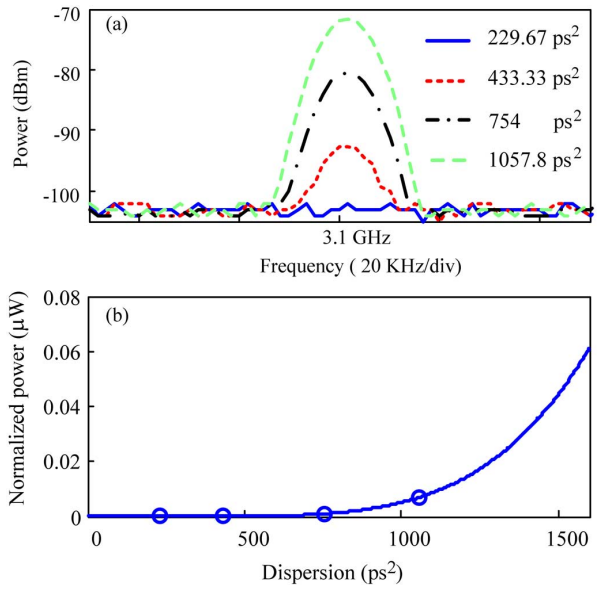

Fig. 18. (a) Measured power spectra and (b) normalized power distribution for the IMP3 in two-tone transmission.

using either a dispersive fiber or an interferometer, is that the system frequency response is periodic. In addition, PM-to-IM conversion using a dispersive fiber or an interferometer has frequency response that has a notch at the dc (i.e., low frequency cut-off). In contrast, an MZM-based MWP system can have a flat frequency response if the chromatic dispersion in the system is completely compensated. In a PM-based MWP system that using dispersion-induced PM-to-IM conversion, according to (11), the central frequency at the first peak of the frequency response is $\omega_0 = \sqrt{\pi/(\beta_2 L)}$ with a 3-dB bandwidth of $\Delta\omega = (\sqrt{5/3} - \sqrt{1/3}) \cdot \omega_0 \approx 0.71\omega_0$. Therefore, the PM-based MWP system should be designed to operate within the 3-dB bandwidth, which means that the fiber length should be carefully chosen to make the MWP system operating in the 3-dB bandwidth. This is the major limitation that should be considered in using a PM-based MWP system with dispersion-induced PM-to-IM conversion.

In conclusion, a unified theoretical framework was developed, for the analysis of PM-based MWP systems for both linear and nonlinear applications. The key advantage of using PM in a MWP system is that the phase modulator is not biased which would eliminate the bias drifting problem in an MZM-based MWP system. Analytical models for single-tone and two-tone transmissions, microwave frequency multiplication, and subcarrier frequency upconversion were derived. The developed models were strict and accurate since all optical sidebands were included in the beating process in the theoretical derivation. Thanks to the use of the addition theory for Bessel functions in the theoretical derivation, the obtained analytical results are compact. The given analytical models were verified by numerical simulations. The analytical models for single-tone and two-tone transmissions were further confirmed by experiments using an SMF with different lengths. The use of the analytical models for the analysis of different MWP systems was also presented. The theoretical findings help to simplify greatly the design and analysis of a PM-based microwave photonic system that is based on the dispersion-induced PM-to-IM conversion.

APPENDIX

We can rewrite the upconverted signal in (28) as

$$\begin{aligned} & i_{k\omega_{\rm LO}+\omega_{\rm IF}}(t) \\ &= \sum_{n=-\infty}^{\infty} \left\{ \Gamma^*_{n\omega_{\rm LO}} \Gamma_{(n+k)\omega_{\rm LO}+\omega_{\rm IF}} + \Gamma_{(n+k)\omega_{\rm LO}} \Gamma^*_{n\omega_{\rm LO}-\omega_{\rm IF}} \right\} \\ &= A + B \end{aligned} \tag{A1}$$

where

$$\begin{aligned} A &= \sum_{n=-\infty}^{\infty} \Gamma^*_{n\omega_{\rm LO}} \Gamma_{(n+k)\omega_{\rm LO}+\omega_{\rm IF}} \\ &= \sum_{n=-\infty}^{\infty} \left\{ \frac{m_1}{2} j^k J_n(m_2) J_{n-k}(m_2) \exp[j(k\omega_{\rm LO} + \omega_{\rm IF})t] \right. \\ &\quad \times \exp\left[-j\frac{1}{2}\beta_2 L \left(k^2\omega_{\rm LO}^2 + \omega_{\rm IF}^2\right) \right] \\ &\quad \times \exp\left[j\frac{1}{2}\beta_2 L 2nk\omega_{\rm LO}^2 \right] \\ &\quad \left. \times \exp\left[j\frac{1}{2}\beta_2 L 2(n-k)\omega_{\rm LO}\omega_{\rm IF} \right] \right\} \end{aligned} \tag{A2}$$

and

$$\begin{aligned} B &= \sum_{n=-\infty}^{\infty} \Gamma_{(n+k)\omega_{\rm LO}} \Gamma^*_{n\omega_{\rm LO}-\omega_{\rm IF}} \\ &= \sum_{n=-\infty}^{\infty} \left\{ \frac{m_1}{2} j^k J_n(m_2) J_{n+k}(m_2) \exp[j(k\omega_{\rm LO} + \omega_{\rm IF})t] \right. \\ &\quad \times \exp\left[j\frac{1}{2}\beta_2 L \left(k^2\omega_{\rm LO}^2 + \omega_{\rm IF}^2\right) \right] \\ &\quad \times \exp\left[j\frac{1}{2}\beta_2 L 2nk\omega_{\rm LO}^2 \right] \\ &\quad \left. \times \exp\left[j\frac{1}{2}\beta_2 L 2(n+k)\omega_{\rm LO}\omega_{\rm IF} \right] \right\}. \end{aligned} \tag{A3}$$

According to the addition theorem, we can obtain

$$A = \xi_1 J_{-k}(R) \exp(-jk\Omega) \tag{A4}$$

$$B = \xi_2 J_k(R) \exp(jk\Omega) \tag{A5}$$

where in (A4) and (A5)

$$\begin{aligned} \xi_1 &= (m_1/2) j^k \exp\left[-j\beta_2 L \left(k^2\omega_{\rm LO}^2 + \omega_{\rm IF}^2\right)/2 \right] \\ \xi_2 &= (m_1/2) j^k \exp\left[j\frac{1}{2}\beta_2 L \left(k^2\omega_{\rm LO}^2 + \omega_{\rm IF}^2\right)/2 \right] \\ R &= 2m_2 \sin\left[\beta_2 L \left(\omega_{\rm LO}\omega_{\rm IF} + k\omega_{\rm LO}^2\right)/2 \right] \\ \Omega &= \pi/2 + \beta_2 L \left(\omega_{\rm LO}\omega_{\rm IF} + k\omega_{\rm LO}^2\right)/2 - \beta_2 L k\omega_{\rm LO}^2. \end{aligned}$$

Therefore, according to (A1), (A4), and (A5) we can obtain

$$\begin{aligned} i_{k\omega_{\rm LO}+\omega_{\rm IF}}(t) &= A + B \\ &= (-1)^k m_1 \cos\left[\frac{1}{2}\beta_2 L \left(k\omega_{\rm LO}\omega_{\rm IF} + \omega_{\rm IF}^2\right) \right] \\ &\quad \times J_k(R) \cdot \exp[j(k\omega_{\rm LO} + \omega_{\rm IF})t]. \end{aligned} \tag{A6}$$

REFERENCES

[1] A. J. Seeds, "Microwave photonics," *IEEE Trans. Microw. Theory Tech.*, vol. 50, no. 3, pp. 877–887, Mar. 2002.

[2] B. M. Haas and T. E. Murphy, "A simple, linearized, phase-modulated analog optical transmission system," *IEEE Photon. Technol. Lett.*, vol. 19, no. 10, pp. 729–731, May 2007.

[3] F. Zeng and J. P. Yao, "All-optical bandpass microwave filter based on an electro-optic phase modulator," *Opt. Exp.*, vol. 12, no. 16, pp. 3814–3819, Aug. 2004.

[4] G. Ning, S. Aditya, P. Shum, L. H. Cheng, Y. D. Gong, and C. Lu, "Tunable photonic microwave bandpass filter using phase modulation and a chirped fiber grating in a Sagnac loop," *IEEE Photon. Technol. Lett.*, vol. 17, no. 9, pp. 1935–1937, Sep. 2005.

[5] J. Wang, F. Zeng, and J. P. Yao, "All-optical microwave bandpass filter with negative coefficients based on PM-IM conversion," *IEEE Photon. Technol. Lett.*, vol. 17, no. 10, pp. 2176–21780, Oct. 2005.

[6] G. Qi, J. P. Yao, J. Seregelyi, C. Bélisle, and S. Paquet, "Optical generation and distribution of continuously tunable millimeter-wave signals using an optical phase modulator," *J. Lightw. Technol.*, vol. 23, no. 9, pp. 2687–2695, Sep. 2005.

[7] J. P. Yao, G. Maury, Y. L. Guennec, and B. Cabon, "All-optical subcarrier frequency conversion using an electrooptic phase modulator," *IEEE Photon. Technol. Lett.*, vol. 17, no. 11, pp. 2427–2429, Nov. 2005.

[8] Y. Le Guennec, G. Maury, J. P. Yao, and B. Cabon, "New optical microwave up-conversion solution in radio-over-fiber networks for 60 GHz wireless applications," *J. Lightw. Technol.*, vol. 24, no. 3, pp. 1277–1282, Mar. 2006.

[9] M. J. LaGasse and S. Thaniyavarn, "Bias-free high-dynamic-range phase-modulated fiber-optic link," *IEEE Photon. Technol. Lett.*, vol. 9, no. 5, pp. 681–683, May 1997.

[10] J. Marti, F. Ramo, V. Polo, M. Fuster, and J. L. Corral, "Millimeter-wave signal generation and harmonic upconversion through PM-IM Conversion in Chirped Fiber Gratings," *Fiber Integr. Opt.*, vol. 19, no. 2, pp. 187–198, 2000.

[11] J. Yu, Z. Jia, L. Xu, L. Chen, T. Wang, and G.-K. Chang, "DWDM optical millimeter-wave generation for radio-over-fiber using an optical phase modulator and an optical interleaver," *IEEE Photon. Technol. Lett.*, vol. 18, no. 13, pp. 1418–1420, Jul. 2006.

[12] F. Zeng and J. P. Yao, "Investigation of phase modulator based all-optical bandpass microwave filter," *J. Lightw. Technol.*, vol. 23, no. 4, pp. 1721–1728, Apr. 2005.

[13] H. Chi and J. P. Yao, "Power distribution of phase-modulated microwave signals in a dispersive fiber-optic link," *IEEE Photon. Technol. Lett.*, vol. 20, no. 4, pp. 315–317, Feb. 2008.

[14] G. E. Andrews, R. Askey, and R. Roy, *Special Functions*. Cambridge, U.K.: Cambridge Univ. Press, 2001.

[15] V. J. Urick, F. Bucholtz, P. S. Devgan, J. D. McKinney, and K. J. Williams, "Phase modulation with interferometric detection as an alternative to intensity modulation with direct detection for analog-photonic links," *IEEE Trans. Microw. Theory Tech.*, vol. 55, no. 9, pp. 1978–1985, Sep. 2007.

Hao Chi received the Ph.D. degree in electronic engineering from Zhejiang University, Hangzhou, China, in 2001.

He joined the Department of Information and Electronic Engineering, Zhejiang University, in 2003. Before that, he spent half year in the Hong Kong Polytechnic University as a Research Assistant and two years in Shanghai Jiaotong University, Shanghai, China, as a Postdoctoral Fellow. Since June 2006, he has also been with the Microwave Photonics Research Laboratory, School of Information Technology and Engineering, University of Ottawa, Canada. His research interests include optical communications and networking, microwave photonics, fiber-optic sensors, optical signal processing and fiber grating-based components.

Xihua Zou received the B.E. degree in communication engineering in 2003 from Southwest Jiaotong University, Chengdu, China. Currently, he is pursuing his Ph.D. degree under the Joint Ph.D. Training Program sponsored by Chinese Scholarships Council in the University of Ottawa, Ottawa, Canada and the Southwest Jiaotong University, Chengdu, China.

His current interests include microwave photonics, optical pulse generation and compression, fiber Bragg gratings, and passive fiber devices for optical fiber communication system.

Jianping Yao (M'99–SM'01) received the Ph.D. degree in electrical engineering from the Université de Toulon, France, in 1997.

He joined the School of Information Technology and Engineering, University of Ottawa, Ontario, Canada, in 2001, where he is a Professor and University Research Chair, Director of the Microwave Photonics Research Laboratory, and Director of the Ottawa-Carleton Institute for Electrical and Computer Engineering. He holds a Yongqian Endowed Chair Professorship of Zhejiang University since May 2008, China. From 1999 to 2001, he held a faculty position in the School of Electrical and Electronic Engineering, Nanyang Technological University, Singapore. He spent three months as an Invited Professor in the Institut National Polytechnique de Grenoble, France, in 2005. He established the Microwave Photonics Research Laboratory at the University of Ottawa in 2002. His research has focused on microwave photonics, which includes photonic processing of microwave signals, photonic generation of microwave, mm-wave and THz, radio over fiber, UWB over fiber, and optically controlled phased array antenna. His research also covers fiber optics, which includes fiber lasers, fiber and waveguide Bragg gratings, fiber-optic sensors and bio-photonics. He has authored or co-authored 220 papers in refereed journals and in conference proceedings.

Dr. Yao is an Associate Editor of the *International Journal of Microwave and Optical Technology*. He is on the Editorial Board of IEEE TRANSACTIONS ON MICROWAVE THEORY AND TECHNIQUES. He is a chair or committee member of numerous international conferences, symposia and workshops. He received the 2005 International Creative Research Award of the University of Ottawa. He was the recipient of the 2007 George S. Glinski Award for Excellence in Research. He was named University Research Chair in Microwave Photonics in 2007 and was awarded one of NSERC's one hundred Discovery Accelerator Supplements in 2008. He is a registered professional engineer of Ontario. He is a Member of SPIE, OSA, and a Senior Member of IEEE LEOS and IEEE MTT Societies.